

Brain region specificity in reactive oxygen species production and maintenance of redox balance

Andrey Y. Vinokurov¹, Olga A. Stelmashuk¹, Polina A. Ukolova¹, Evgeny A. Zherebtsov^{1,2}, Andrey Y. Abramov^{1, 3,*}

¹Cell Physiology and Pathology Laboratory, Orel State University, Orel, 302026, Russia

²Optoelectronics and Measurement Techniques Laboratory, University of Oulu, Oulu, 90014, Finland

³Department of Clinical and Movement Neurosciences, UCL Queen Square Institute of Neurology, Queen Square, London WC1N 3BG, UK

Abstract

The brain produces various reactive oxygen species in enzymatic and non-enzymatic reactions as a by-product of metabolism and/or for redox signaling. Effective antioxidant system in the brain cells maintains redox balance. However, neurons and glia from some brain regions are more vulnerable to oxidative stress in ischaemia/reperfusion, epilepsy, and neurodegenerative disorders than the rest of the brain. Using live cell imaging, we have measured the rate of cytosolic and mitochondrial reactive oxygen species production, lipid peroxidation, and glutathione levels in cortex, hippocampus, midbrain, brain stem and cerebellum in acute slices of rat brain. We have found that the basal rate of ROS production is at its highest in brain stem and cerebellum, and that it is mainly generated by glial cells. Activation of neurons and glia by glutamate and ATP led to maximal rates of ROS production in the midbrain compared to the rest of the brain. Mitochondrial ROS had only minor implication to the total ROS production with maximal values in the cortex and minimal in the midbrain. The basal rate of lipid peroxidation was higher in the midbrain and hippocampus, while the GSH level was similar in most brain regions with the lowest level in the midbrain. Thus, the rate of ROS production, lipid peroxidation and the level of GSH vary across brain regions.

Keywords: brain regions, neurons, astrocytes, reactive oxygen species, mitochondria, GSH

Abbreviations: ROS, reactive oxygen species; MAO, monoamine oxidase; GSH, glutathione; HBSS, Hanks' balanced salt solution; HET, dihydroetidium; MCB, monochlorobimane

* Corresponding author. Department of Clinical and Movement Neurosciences, UCL Queen Square Institute of Neurology, Queens Square, London, WC1N 3BG, UK.

E-mail address: a.abramov@ucl.ac.uk (A.Y. Abramov).

1. Introduction

The brain is the part of the central nervous system which regulates almost all processes in the whole body. Brain produces and consumes more energy than any other organ or tissue and takes up almost 10 times more glucose, oxygen, and lipids. All these factors dramatically increase the chances of producing free radicals, including reactive oxygen species (ROS) in this organ. To protect itself from oxidative damage by sufficient antioxidant system, the brain consumes energy from different sources, mostly glucose, for maintenance of the redox balance in the neuronal and glial cells [1,2].

In brain cells, ROS are constantly produced in the electron transport chain of mitochondria and in multiple enzymes in response to a pathological or physiological stimulus. Thus, monoamine oxidase (MAO A and MAO B) utilise catecholamines and produce hydrogen peroxide as a part of the signalling mechanism [3,4]. Activation of NADPH oxidases can be triggered by ischemia, seizures, misfolded proteins but also can be stimulated by the physiology of the glutaminergic system [5–9].

Brain regions are specialised for distinctive function, and because of it, the metabolic rate and signalling intensity can vary [10,11]. The level of endogenous antioxidants (such a glutathione (GSH) is also dependent on the rate of metabolic activity and free radical production. Considering this, the level of GSH could also be different, not only between cell types, but also between brain regions [12,13]. Importantly, the level of antioxidants, including GSH in different brain regions, may change dramatically in the time of physical activity and because of toxicity [14].

Although the increased level of lipid peroxidation is a marker for oxidative stress, oxidised lipids and products of lipid peroxidation such as 4-HNE, could also play a signalling role [15,16].

Oxidative stress was shown to be one of the triggers in the mechanism of neurodegeneration in Parkinson's disease, Alzheimer's disease, and a number of other neurological disorders [17,18]. However, it is not clear why specific regions are more vulnerable to oxidative damage than others. One of the possible explanations could be an enhanced rate of ROS production in specific regions or a lower level of GSH.

Here, we studied the rates of ROS production in cytosol or mitochondria, the rate of lipid peroxidation and GSH level in neurons and astrocytes in different brain regions of acute brain slices. We have found that ROS production is different in various brain areas and also depends on the physiological activity of the cells. The most active ROS production was found to take place in the brain stem and the cerebellum, and after

stimulation with neuro- and gliotransmitters - in the midbrain. In the resting conditions, mitochondria had only a minor impact on total ROS production with maximal values in the cortex.

2. Materials and methods

2.1. Acute brain slices

All the manipulations with animals were approved by the Institutional ethical committee of Orel State University (Minutes No. 18 dated 21.02.2020) in compliance with Russian Federation legislation. For the experiments, 12-weeks male Wistar rats (250-300 g) (17 for all preparations) were used. Condition for keeping animals included a 12-hr light cycle and *ad libitum* access to water and food. The animals were killed by cervical dislocation. After extraction, the brain was placed in Hanks' balanced salt solution (HBSS) (pH 7.4/4°C). Slices of brain regions (cortex, midbrain, cerebellum, brainstem, hippocampus) with a thickness of 500 µm were obtained according to the standard protocol [19] and kept before experiments in HBSS (pH 7.4/37°C) with moderate oxygenation.

2.2. ROS production, lipid peroxidation rate, reduced glutathione measurements in acute brain slices

To measure the total cell ROS production and reduced glutathione content was used the setup in two versions: with LED M455F1 (Thorlabs Inc., USA) for excitation of fluorescence of the dihydroethidium (HEt) oxidation products or with BDL-SMN-375 laser source (Becker & Hickl) for excitation of fluorescence of the conjugation product in the reaction between monochlorobimane (MCB) and reduced glutathione. In this system, the excitation radiation through the optical fiber passes through the collimator and the band-pass filter (when using LED M455F1), and then, through the beam splitting filter plate and the lens is directed to the studied area. Emitted fluorescence light was reflected through a 416 nm (in the configuration for reduced glutathione measurements) or 490 nm long-pass filters (in the configuration for HEt) to a highly sensitive DCC 3260C cooling CCD camera (Thorlabs et al., USA). The field of view of the camera on the sample is a rectangular section with an area of about 1 mm². To avoid the accumulation of oxidised products, dihydroethidium was not pre-loaded to the slices but was added during the experiments (in the final concentration of 5 µM) after the period of fluorescence basal level measurements. For the glutathione levels determination, slices were pre-loaded with 50 µM MCB solution.

The fluorescence intensity of the conjugation product between reduced glutathione and MCB was measured on 5 images from every slice.

2.3. *Live cell imaging*

For the determination of ROS production rate in neurons and glial cells, mitochondrial ROS production rate and rate of lipid peroxidation Zeiss 900 Laser Scanning Microscope was used. ROS production rate in neurons and glial cells was measured after 10 min incubation of slices in 5 μ M solution of HET in HBSS (pH 7.4/37°C). ROS production in glial cells was activated by adding ATP (100 μ M) and in neurons – by the addition of L-glutamate (20 μ M). Mitochondrial ROS production rate was performed with MitoTracker Red CM-H2Xros. Slices were incubated for 10 minutes in 5 μ M solution of the probe; after that, confocal images were obtained in 5 fields of view from every slice (objective 20x).

Lipid peroxidation. Lipid peroxidation was measured with 11-BODIPY 581/591 with excitation by lasers 481 nm and 561 nm and detection from 505 nm to 550 nm and above 580 nm (objective 20x). The results are presented as fluorescence intensity ratio 581/591.

3. Results

3.1 *Cerebellum and brainstem have the highest rates of ROS production*

The basal rate of ROS production in various brain region was assessed using fluorescent indicator HET (Figure 1A). Although this indicator can interact with different forms of free radicals, it is mainly oxidized by superoxide anion [20,21].

The rates of ROS production in acute brain slices from the various regions were significantly different (Figure 1 A-G). The lowest rate was observed in the cortex area (Figure 1 B, G), while in the neighboring hippocampal area, the rate of ROS production was 3-fold higher ($291 \pm 124\%$ of cortical, N=9 experiments; Figure 1 C, G). Brain stem areas were characterized by the highest rate of ROS production ($699.2 \pm 91.6\%$, N=9 sections; Figure 1 F, G), 1.8 times higher than the rates for the cerebellum ($398.0 \pm 78.3\%$ of cortical, N=3 rats, n=9 slices; Figure 1 A, E, G). Thus, the basal rates of ROS production, which should correspond to resting functional activity in the cells, are dramatically different between brain regions. The difference in the rate of ROS production could be explained by a number of factors, including astrocytes/neurons ratio, functional activity of the cells etc.

3.2 *Differences in generation of ROS between brain regions are dependent on glia*

To identify how activation of the glial cells and neurons can change the maximal rate of ROS production, we applied 100 μ M ATP, which mainly activates astrocytes through purinergic receptors and the neurotransmitter glutamate (20 μ M) to stimulate neurons [22]. ATP and glutamate could stimulate calcium signal in astrocytes and neurons and, for both neurotransmitters, it has been reported the ability to activate ROS production through the NADPH oxidase [23,24].

In agreement of the text books and the images shown in Figure 2 A, the examined sections of the brain regions were morphologically heterogeneous and characterized by the presence of zones with a higher content of glial or neuronal cells.

The basal rate of ROS production in neurons or glial cells was identified using the rate of increase of Het fluorescence before stimulation in the areas which were specifically activated by ATP or glutamate (Figure 2A). Interestingly, the dramatic differences in the basal rate of ROS, which we found in the wide field areas of brain regions (Figure 1) was observed only in cells that responded to ATP, but not in neurons (cells with response to glutamate Figure 2A, B-F, G, H).

3.3 ATP and glutamate induce highest rate of ROS in midbrain

Expectably, the application of ATP or glutamate led to a significant increase in the rate of HET fluorescence (Figure 2 B-F) compared to basal rates in the same regions. The most profound 5-fold increase was observed in the midbrain ($495.3 \pm 70.0\%$; Figure 2 J) in glial cells (ATP stimulation) and 4-fold increase ($386.7 \pm 44.9\%$; Figure 2 K) in neurons (glutamate stimulation, N=4 rats, n=8 slices). Activation of the ROS production in the rest of the regions was characterized by ~ 2-3-fold increase in response to ATP (for the cortex, hippocampus, cerebellum and brain stem, respectively: $206.4 \pm 25.4\%$, $262.1 \pm 53.0\%$, $283.9 \pm 55.1\%$, $243.0 \pm 53.9\%$, N=4 rats, n=8 slices; Figure 2 J) and to glutamate for the cortex, hippocampus, cerebellum and brain stem, respectively: $206.8 \pm 39.9\%$, $282.7 \pm 62.1\%$, $292.7 \pm 75.7\%$, $240.5 \pm 57.1\%$, N=4 rats, n=8 slices (Figure 2K).

Data presented in the histograms Figure 2 J, K help to compare the values of increase in the ROS production in this particular field but does not allow to compare the activated ROS production between regions. We normalized the data to the basal rate of ROS production from the cortex and found that the increase in the rate of fluorescence in response to ATP was diminishing in the sequence "cerebellum – midbrain - brain stem - hippocampus - cortex" (respectively $450.5 \pm 87.5\%$; $432.2 \pm 61.1\%$, $297.2 \pm 65.9\%$, $290.5 \pm 58.7\%$, $206.4 \pm 25.4\%$, N=4 rats, n=8 slices; Figure 2L), and in response to glutamate -in the sequence "midbrain - hippocampus - cerebellum - brain stem - cortex"

respectively $478.1 \pm 55.6\%$, $428.8 \pm 94.3\%$, $377.7 \pm 97.6\%$, $250.1 \pm 59.4\%$, $206.8 \pm 39.9\%$, N=4 rats, n=8 slices; Figure 2 M.

Thus, higher ROS production levels in the brain stem and cerebellum are more likely to be explained by activated glial cells in these regions. However, the maximal stimulation of ROS production was observed in response to ATP or glutamate was observed in the midbrain, suggesting the higher importance of redox signaling in this brain area.

3.4 Basal rate of mitochondrial ROS production is highest in cortex

Mitochondria are one of the major sources of ROS production of the cells in resting conditions. The level of ROS production in the electron transport chain (ETC) of mitochondria is dependent on the metabolic state and the number of other factors, including oxygen level, calcium signal, toxins etc. [25]. To assess the production of mitochondrial ROS in acute brain slices, we used fluorescent probe MitoTracker Red CM-H2Xros (Figure 3A).

We have found that the rate of ROS production in the matrix of mitochondria was highest in the cortex area from acute brain slices (taken as 100%; Figure 3A, B). Mitochondrial ROS production in hippocampus, cerebellum and brainstem was significantly lower ($72.8 \pm 3.8\%$, $67.3 \pm 6.2\%$, $76.7 \pm 4.1\%$ of cortical values respectively, N=5 rats, n=10 slices; Figure 3A, B). The lowest rate of mitochondrial ROS production was found in the midbrain ($35.3 \pm 2.1\%$ of the level of the cortex, N=5 rats, n=10 slices). Interestingly, recently we found that mitochondria in cells from cortical slices had the lowest mitochondrial membrane potential compared to other brain regions and midbrain cells showed the highest metabolic activity [10]. Our results indicate that mitochondrial ROS have only a minor impact on the ROS production in neurons and astrocytes *ex vivo*.

3.5 The hippocampus and midbrain are characterized by the highest rates of lipid peroxidation

Lipid peroxidation is one of the hallmarks of oxidative stress. However, lipid peroxidation and lipid peroxidation products play an important role in cell homeostasis and signalling [26,27]. Although the lipid peroxidation level in brain cells depends on the rate of lipid metabolism, endogenous vitamin E content, activity of phospholipases, it can be activated by ROS production. Therefore, we measured the rate of lipid peroxidation in the acute brain slices using a fluorescent probe C11 BODIPY 581/591 (Figure 4 A).

The rate of lipid peroxidation was most pronounced in the midbrain and hippocampus from acute brain slices ($250.7 \pm 45.0\%$ and $230.8 \pm 24.7\%$ of the level of cortical slices respectively, n=6 slices; Figure 4 A-C). Lower and approximately equal

values were obtained for the cerebellum and brainstem ($100.1 \pm 11.4\%$ and $136.4 \pm 15.8\%$ of cortical level, $n=6$ slices: Figure 4 A-C).

Interestingly, the highest level of lipid peroxidation in the midbrain was not comparable with the relatively low basal rate of ROS production in this brain region (Figures 1-2). However, cells from this region had the highest ROS production in response to a stimulus (Figure 2) and the highest mitochondrial metabolic rate compared to other brain regions [10].

3.6 GSH is lower in midbrain and cerebellum

The maintenance of GSH levels, the main endogenous antioxidant in the brain, is dependent on the multiple enzymes and the neuron-glia interactions [28].

Measurements of GSH in brain slices using MCB as fluorescent indicator showed that there was no difference in the levels of GSH between hippocampus, brain stem and cortex, ($102.7 \pm 4.8\%$ and $100.9 \pm 3.9\%$ of cortical values respectively; $N=3$ rats, $n=12$ slices; Figure 5 A-B), while the midbrain and the cerebellum had a significantly lower levels of GSH ($85.6 \pm 4.1\%$ and $56.4 \pm 1.3\%$ respectively of the level of the cortex, $N=3$ rats, $n=12$ slices; Figure 5 A-B).

4 Discussion

Here we found that the production of ROS in the brain is not distributed equally throughout the brain. The highest rate in resting conditions was in the brain stem and cerebellum areas. Interestingly, this effect was mainly dependent on the ROS production in glial cells, and ROS production in neurons from the same brain areas was not higher than other parts of the brain. ROS production was not associated with higher number of glial cells in these regions – the glia/neuron ratio in cerebellum is lower than in cortex [29] and more likely dependent on the more intensive functional activity of glia in the acute slices of these brain regions compared to the cortex, midbrain and hippocampus. It was also been confirmed by experiments with stimulation of the ROS production by physiological neuro- and gliotransmitters – glutamate and ATP. After stimulation, ROS production in brain stem and cerebellum was even lower compared to other brain regions.

The maximal ROS production in activated neurons and glia in the midbrain was found to be much higher compared to other studied brain regions (Figure 2). Although glutamate and ATP could activate ROS production in various enzymes, including mitochondria – [30], they mainly activate the NADPH oxidase [24,31]. More profound activation of NADPH oxidase in the midbrain, compared to other brain regions, could be

explained by higher expression of this enzyme or by better activation of this enzyme to the L-glutamate and ATP in this brain area.

Mitochondria is accepted to be one of the main producers of ROS in brain cells [25]. Our data suggest that mitochondria in resting conditions have only a minor impact on the total ROS production and have almost no effect on the level of GSH or lipid peroxidation. The level of ROS production in the matrix of mitochondria was lower in the areas with high intracellular production of superoxide. Interestingly, that brain area which is the most sensitive to mitochondrial toxins and the most vulnerable to mitochondrial mutations [32,33] – the midbrain- had the lowest ROS production rates in resting conditions. However, activation of ROS production in mitochondria in this area combined with high intracellular ROS production could trigger oxidative stress.

Lower level of GSH was found in the midbrain and cerebellum compared to the other studied brain regions. Astrocytes play an important role in the production of GSH in the brain and a lower level of GSH in cerebellum and midbrain could be a reflection of the lower proportion of glial to neuronal cells in these areas of the brain [34], but also can be associated with differences in metabolic rates and rates of GSH production in these brain areas.

Our results on lipid peroxidation measurements in *ex vivo* slices from various brain regions showed no correlation between the level of ROS production in cytosol and/or mitochondria and the rate of lipid peroxidation in the same areas (Figure 4). This suggests that the difference in lipid peroxidation rates between brain regions could be more dependent on the rate of lipid metabolism and the level of endogenous antioxidants, and the activity of phospholipases, rather than on oxidation induced by higher levels of ROS in the cells.

Conflict of interest:

The authors declare no conflict of interest.

Acknowledgements

This work was supported by the grant of the Russian Federation Government no. 075-15-2019-1877.

References

- [1] P. Rodriguez-Rodriguez, E. Fernandez, J.P. Bolaños, Underestimation of the pentose-phosphate pathway in intact primary neurons as revealed by metabolic flux analysis, *J. Cereb. Blood Flow Metab.* 33 (2013) 1843–1845.

<https://doi.org/10.1038/jcbfm.2013.168>.

- [2] J.P. Bolaños, Bioenergetics and redox adaptations of astrocytes to neuronal activity, *J. Neurochem.* 139 (2016) 115–125. <https://doi.org/10.1111/jnc.13486>.
- [3] A. Vaarmann, S. Gandhi, A.Y. Abramov, Dopamine induces Ca²⁺ signaling in astrocytes through reactive oxygen species generated by monoamine oxidase, *J. Biol. Chem.* 285 (2010) 25018–25023. <https://doi.org/10.1074/jbc.M110.111450>.
- [4] M. Yamato, W. Kudo, T. Shiba, K.I. Yamada, T. Watanabe, H. Utsumi, Determination of reactive oxygen species associated with the degeneration of dopaminergic neurons during dopamine metabolism, *Free Radic. Res.* 44 (2010) 249–257. <https://doi.org/10.3109/10715760903456084>.
- [5] A.Y. Abramov, L. Canevari, M.R. Duchen, β -Amyloid Peptides Induce Mitochondrial Dysfunction and Oxidative Stress in Astrocytes and Death of Neurons through Activation of NADPH Oxidase, *J. Neurosci.* 24 (2004) 565–575. <https://doi.org/10.1523/JNEUROSCI.4042-03.2004>.
- [6] A.Y. Abramov, A. Scorziello, M.R. Duchen, Three distinct mechanisms generate oxygen free radicals in neurons and contribute to cell death during anoxia and reoxygenation, *J. Neurosci.* 27 (2007) 1129–1138. <https://doi.org/10.1523/JNEUROSCI.4468-06.2007>.
- [7] S. Kovac, A.M. Domijan, M.C. Walker, A.Y. Abramov, Seizure activity results in calcium- and mitochondriaindependent ros production via nadph and xanthine oxidase activation, *Cell Death Dis.* 5 (2014) e1442–e1442. <https://doi.org/10.1038/cddis.2014.390>.
- [8] J. Wang, R.A. Swanson, Superoxide and Non-ionotropic Signaling in Neuronal Excitotoxicity, *Front. Neurosci.* 4 (2020) 861. <https://doi.org/10.3389/fnins.2020.00861>.
- [9] L. Bao, M. V. Avshalumov, J.C. Patel, C.R. Lee, E.W. Miller, C.J. Chang, M.E. Rice, Mitochondria are the source of hydrogen peroxide for dynamic brain-cell signaling, *J. Neurosci.* 29 (2009) 9002–9010. <https://doi.org/10.1523/JNEUROSCI.1706-09.2009>.
- [10] X.P. Cheng, A.Y. Vinokurov, E.A. Zherebtsov, O.A. Stelmashchuk, P.R. Angelova, N. Esteras, A.Y. Abramov, Variability of mitochondrial energy balance across brain regions, *J. Neurochem.* 157 (2021) 1234–1243. <https://doi.org/10.1111/jnc.15239>.
- [11] A.Y. Abramov, P.R. Angelova, Cellular mechanisms of complex I-associated pathology, *Biochem. Soc. Trans.* 47 (2019) 1963–1969. <https://doi.org/10.1042/BST20191042>.
- [12] J. Hirrlinger, R. Dringen, The cytosolic redox state of astrocytes: Maintenance,

- regulation and functional implications for metabolite trafficking, *Brain Res. Rev.* 63 (2010) 177–188. <https://doi.org/10.1016/j.brainresrev.2009.10.003>.
- [13] T.J. Monks, J.F. Ghersi-Egea, M. Philbert, A.J.L. Cooper, E.A. Lock, Symposium overview: The role of glutathione in neuroprotection and neurotoxicity, *Toxicol. Sci.* 51 (1999) 161–177. <https://doi.org/10.1093/toxsci/51.2.161>.
- [14] R.F. de Souza, S.R.A. de Moraes, R.L. Augusto, A. de Freitas Zanona, D. Matos, F.J. Aidar, B.L. da Silveira Andrade-da-Costa, Endurance training on rodent brain antioxidant capacity: A meta-analysis, *Neurosci. Res.* 145 (2019) 1–9. <https://doi.org/10.1016/j.neures.2018.09.002>.
- [15] W. Łuczaj, A. Gęgotek, E. Skrzydlewska, Antioxidants and HNE in redox homeostasis, *Free Radic. Biol. Med.* 111 (2017) 87–101. <https://doi.org/10.1016/j.freeradbiomed.2016.11.033>.
- [16] P.R. Angelova, N. Esteras, A.Y. Abramov, Mitochondria and lipid peroxidation in the mechanism of neurodegeneration: Finding ways for prevention, *Med. Res. Rev.* 41 (2021) 770–784. <https://doi.org/10.1002/med.21712>.
- [17] S. Gandhi, A.Y. Abramov, Mechanism of oxidative stress in neurodegeneration, *Oxid. Med. Cell. Longev.* 2012 (2012). <https://doi.org/10.1155/2012/428010>.
- [18] P.R. Angelova, A.Y. Abramov, Role of mitochondrial ROS in the brain: from physiology to neurodegeneration, *FEBS Lett.* 592 (2018) 692–702. <https://doi.org/10.1002/1873-3468.12964>.
- [19] I.N. Novikova, A. Manole, E.A. Zherebtsov, D.D. Stavtsev, M.N. Vukolova, A. V. Dunaev, P.R. Angelova, A.Y. Abramov, Adrenaline induces calcium signal in astrocytes and vasoconstriction via activation of monoamine oxidase, *Free Radic. Biol. Med.* 159 (2020) 15–22. <https://doi.org/10.1016/j.freeradbiomed.2020.07.011>.
- [20] R. Michalski, B. Michalowski, A. Sikora, J. Zielonka, B. Kalyanaraman, On the use of fluorescence lifetime imaging and dihydroethidium to detect superoxide in intact animals and ex vivo tissues: A reassessment, *Free Radic. Biol. Med.* 67 (2014) 278–284. <https://doi.org/10.1016/j.freeradbiomed.2013.10.816>.
- [21] H. Zhao, S. Kalivendi, H. Zhang, J. Joseph, K. Nithipatikom, J. Vásquez-Vivar, B. Kalyanaraman, Superoxide reacts with hydroethidine but forms a fluorescent product that is distinctly different from ethidium: Potential implications in intracellular fluorescence detection of superoxide, *Free Radic. Biol. Med.* 34 (2003) 1359–1368. [https://doi.org/10.1016/S0891-5849\(03\)00142-4](https://doi.org/10.1016/S0891-5849(03)00142-4).
- [22] A. V. Berezhnov, E.I. Fedotova, A.I. Sergeev, I.Y. Teplov, A.Y. Abramov, Dopamine controls neuronal spontaneous calcium oscillations via astrocytic signal, *Cell*

Calcium. 94 (2021). <https://doi.org/10.1016/j.ceca.2021.102359>.

- [23] A.Y. Abramov, M.R. Duchen, The role of an astrocytic NADPH oxidase in the neurotoxicity of amyloid beta peptides, *Philos. Trans. R. Soc. B Biol. Sci.* 360 (2005) 2309–2314. <https://doi.org/10.1098/rstb.2005.1766>.
- [24] A.M. Brennan, S. Won Suh, S. Joon Won, P. Narasimhan, T.M. Kauppinen, H. Lee, Y. Edling, P.H. Chan, R.A. Swanson, NADPH oxidase is the primary source of superoxide induced by NMDA receptor activation, *Nat. Neurosci.* 12 (2009) 857–863. <https://doi.org/10.1038/nn.2334>.
- [25] P.R. Angelova, A.Y. Abramov, Functional role of mitochondrial reactive oxygen species in physiology, *Free Radic. Biol. Med.* 100 (2016) 81–85. <https://doi.org/10.1016/j.freeradbiomed.2016.06.005>.
- [26] A.M. Domijan, S. Kovac, A.Y. Abramov, Lipid peroxidation is essential for phospholipase C activity and the inositol-trisphosphate-related Ca²⁺ signal, *J. Cell Sci.* 127 (2014) 21–26. <https://doi.org/10.1242/jcs.138370>.
- [27] G. Cohen, Y. Riahi, V. Sunda, S. Deplano, C. Chatgililoglu, C. Ferreri, N. Kaiser, S. Sasson, Signaling properties of 4-hydroxyalkenals formed by lipid peroxidation in diabetes, *Free Radic. Biol. Med.* 65 (2013) 978–987. <https://doi.org/10.1016/j.freeradbiomed.2013.08.163>.
- [28] R. Dringen, J. Hirrlinger, Glutathione pathways in the brain, *Biol. Chem.* 384 (2003) 505–516. <https://doi.org/10.1515/BC.2003.059>.
- [29] S. Herculano-Houzel, B. Mota, R. Lent, Cellular scaling rules for rodent brains, *Proc. Natl. Acad. Sci. U. S. A.* 103 (2006) 12138–12143. <https://doi.org/10.1073/pnas.0604911103>.
- [30] R. Abeti, A.Y. Abramov, Mitochondrial Ca(2+) in neurodegenerative disorders, *Pharmacol. Res.* 99 (2015) 377–381. <https://doi.org/10.1016/j.phrs.2015.05.007>.
- [31] A.Y. Abramov, J. Jacobson, F. Wientjes, J. Hothersall, L. Canevari, M.R. Duchen, Expression and modulation of an NADPH oxidase in mammalian astrocytes, *J. Neurosci.* 25 (2005) 9176–9184. <https://doi.org/10.1523/JNEUROSCI.1632-05.2005>.
- [32] R. Betarbet, T.B. Sherer, G. MacKenzie, M. Garcia-Osuna, A. V. Panov, J.T. Greenamyre, Chronic systemic pesticide exposure reproduces features of Parkinson's disease, *Nat. Neurosci.* 3 (2000) 1301–1306. <https://doi.org/10.1038/81834>.
- [33] J. Blesa, S. Przedborski, Parkinson's disease: Animal models and dopaminergic cell vulnerability, *Front. Neuroanat.* 8 (2014) 155. <https://doi.org/10.3389/fnana.2014.00155>.

[34] B. Mota, S. Herculano-Houzel, All brains are made of this: A fundamental building block of brain matter with matching neuronal and glial masses, *Front. Neuroanat.* 8 (2014) 127. <https://doi.org/10.3389/fnana.2014.00127>.

Figure Legends

Figure 1. Rate of the ROS production in acute slices from different brain regions. A – image of the Het fluorescence in acute slice of cerebellum. B, C, D, E, F – representative traces of the Het fluorescence in acute slices of cortex, hippocampus, midbrain, cerebellum and brain stem. G- Rate of Het fluorescence in different brain regions normalised to the rate in cortex. The error bars depict mean \pm SEM, The P value was calculated by ANOVA with the Tukey post hoc test. * $p < 0.05$.

Figure 2. Activation of ROS production in different brain regions in response to glutamate and ATP. A- representative confocal images of Het fluorescence in acute brain slices of brain regions. B, C, D, F, E – representative traces of the Het fluorescence in acute brain slices of different brain regions taken from regions with response to 100 μ M ATP or 10 μ M glutamate. Basal rate of Het fluorescence increases from the areas with response to 100 μ M ATP (G) or 10 μ M glutamate (H) measured before ATP and glutamate were added. Data presented as percentage of cortical results. The rate of Het fluorescence after application of 100 μ M ATP or 10 μ M glutamate normalised to basal rate in these areas (I, J) or as percentage of the cortical values (K, L). The error bars depict mean \pm SEM, The P value was calculated by ANOVA with the Tukey post hoc test. * $p < 0.05$. ** $p < 0.01$; *** $p < 0.001$.

Figure 3. Production of ROS in mitochondria of the cells from acute brain slices from different brain regions. A- representative confocal images of MitoTracker Red CMXROS from different brain regions. B- The rate of Mito Tracker Red CMXROS fluorescence measured in different brain regions. Data presented as percentage of cortical values. The error bars depict mean \pm SEM, The P value was calculated by ANOVA with the Tukey post hoc test. * $p < 0.05$.

Figure 4. The rate of lipid peroxidation in acute slices from different brain regions. A- Representative images of C-11 BODYPI from acute brain slices of different brain regions. B- Typical traces of C-11 BODYPI fluorescence (560 nm/488 nm ratio) from acute brain slices of different brain regions. C- quantification of the rate of C-11 BODYPI fluorescence (560 nm/488 nm ratio) in acute slices from different brain regions. Data presented as percentage of cortical values. The error bars depict mean \pm SEM, The P

value was calculated by ANOVA with the Tukey post hoc test. * $p < 0.05$.

Figure 5. The level of GSH in acute brain slices of different brain regions. A- Wide field images of MCB fluorescence of acute brain slices of different brain regions. B- The level of MCB fluorescence in acute brain slices of different brain regions. Data presented as percentage of cortical values. The error bars depict mean \pm SEM, The P value was calculated by ANOVA with the Tukey post hoc test. * $p < 0.05$.

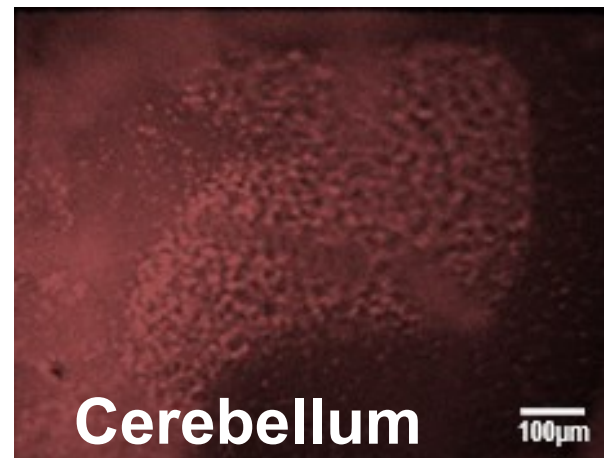
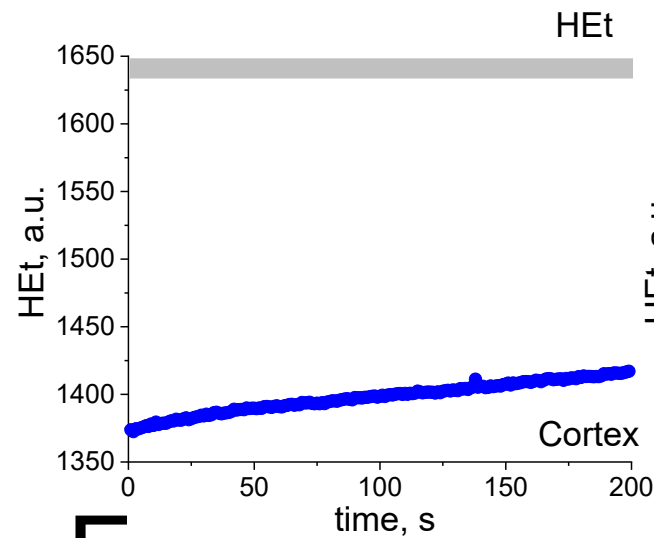
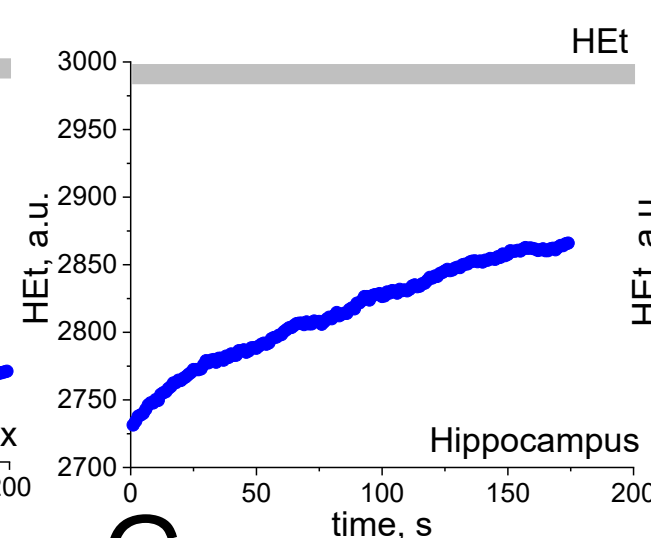
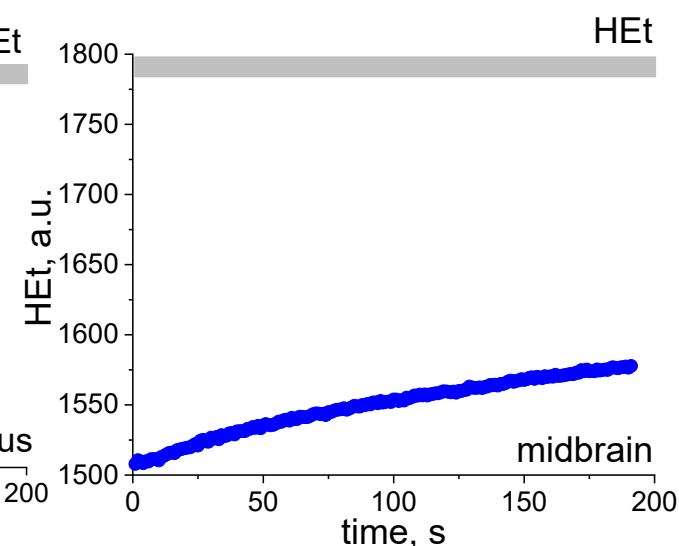
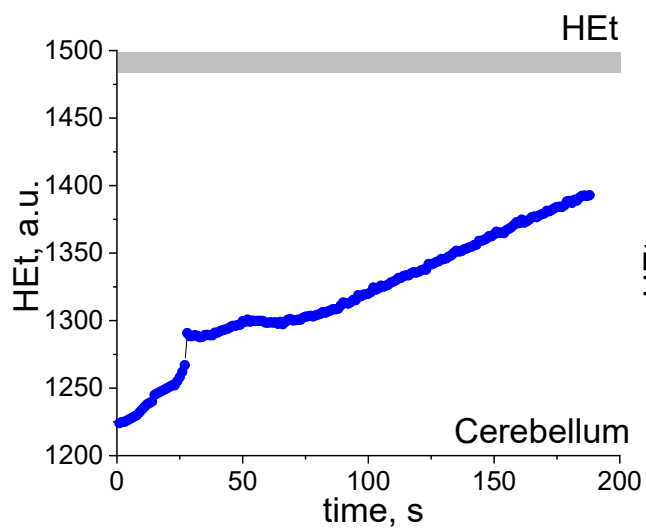
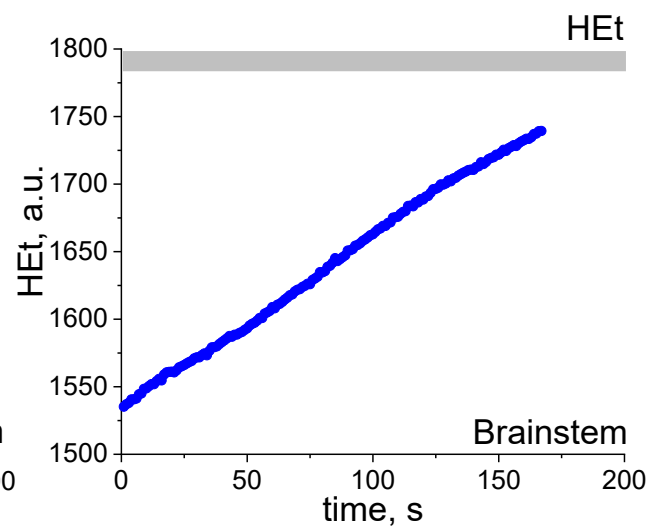
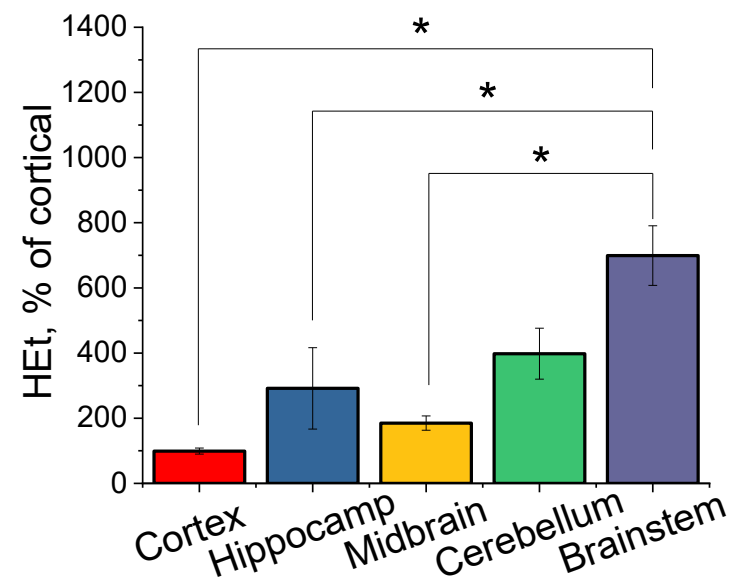
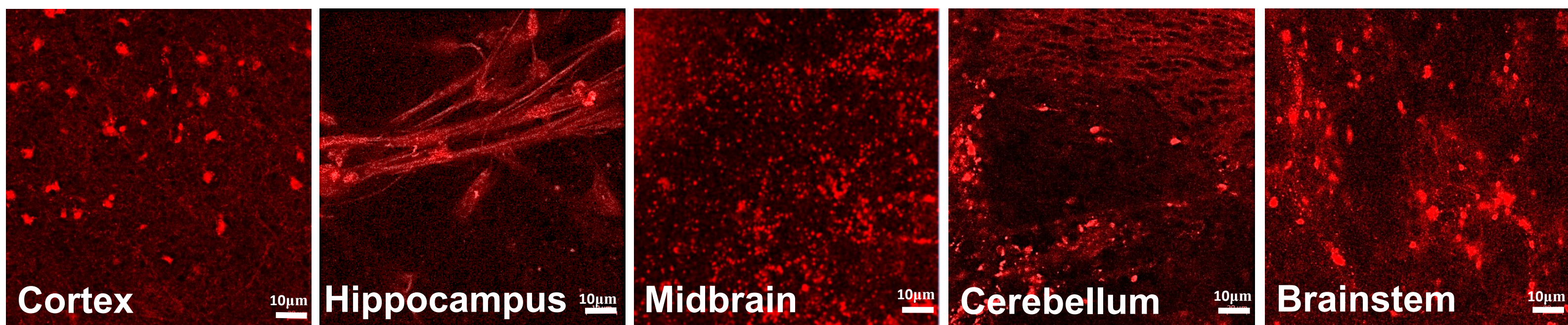
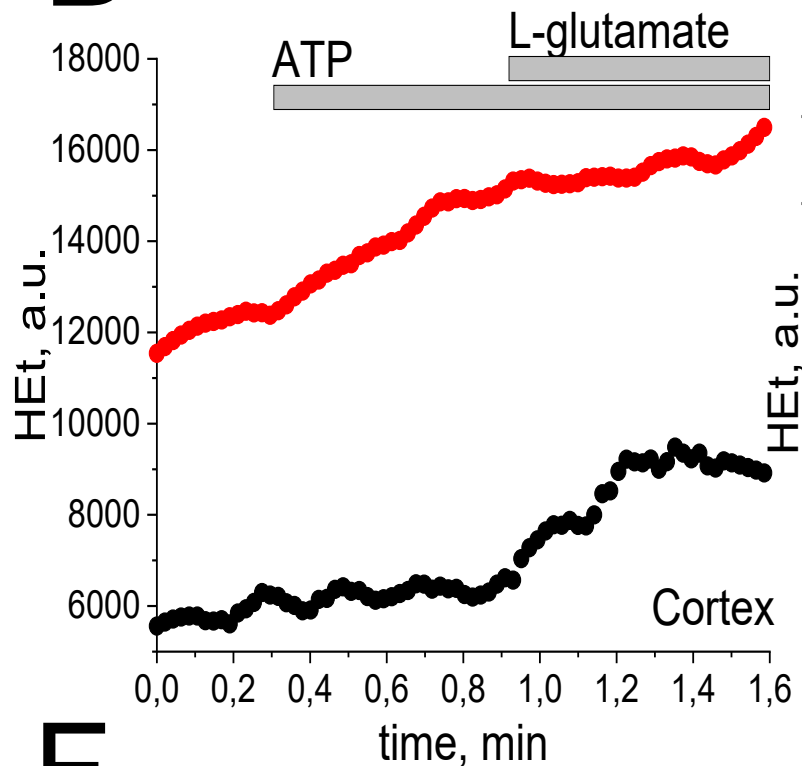
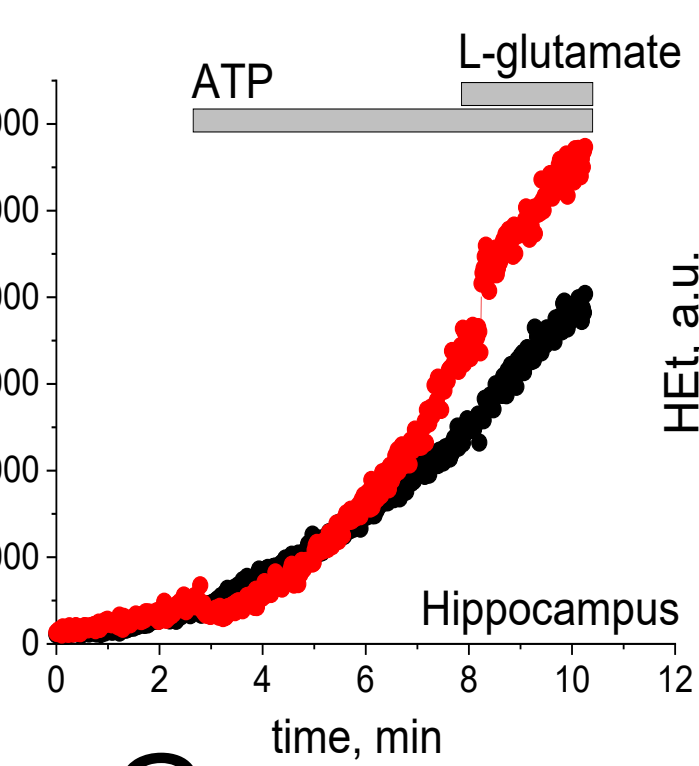
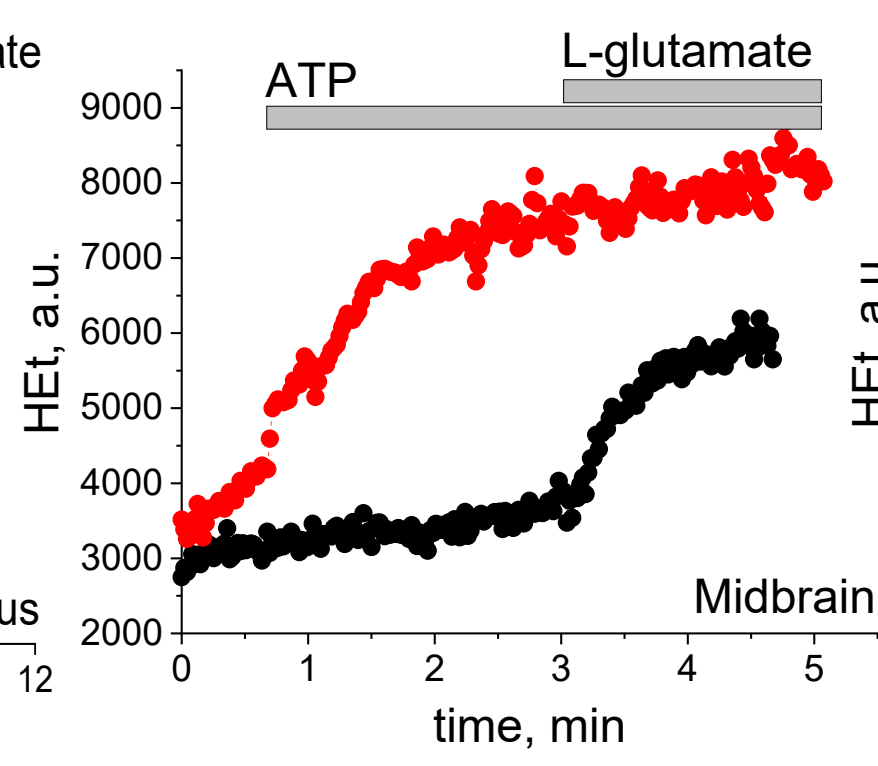
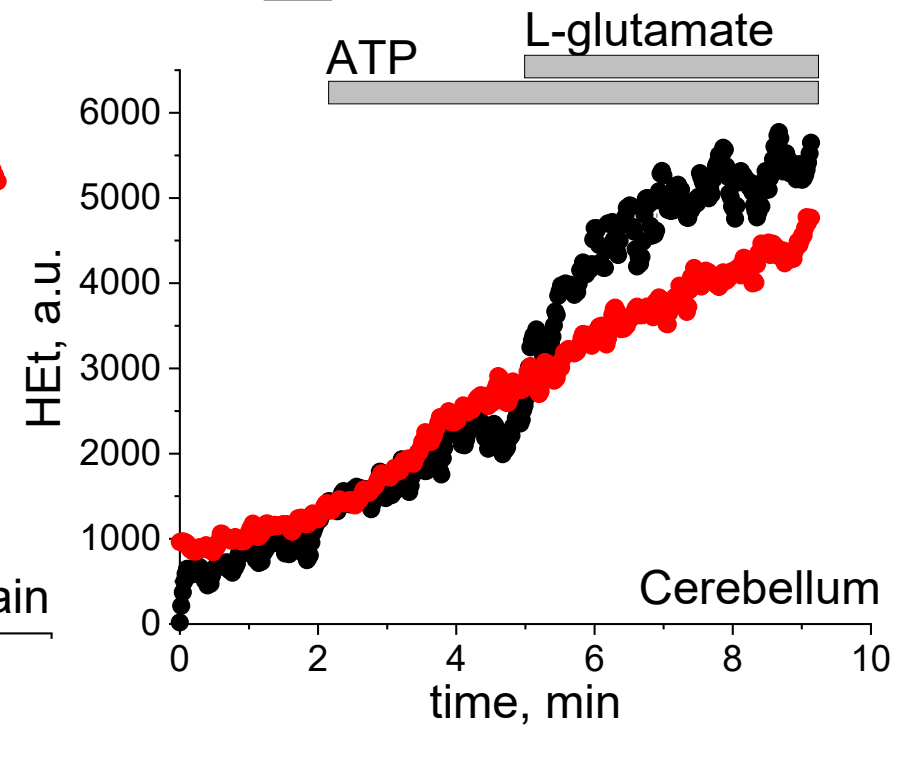
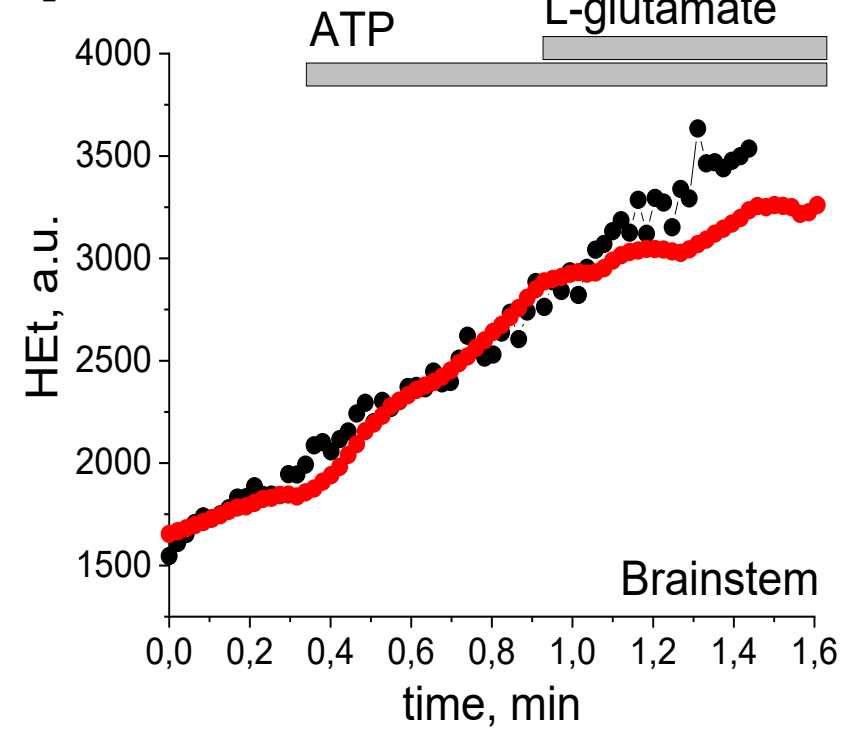
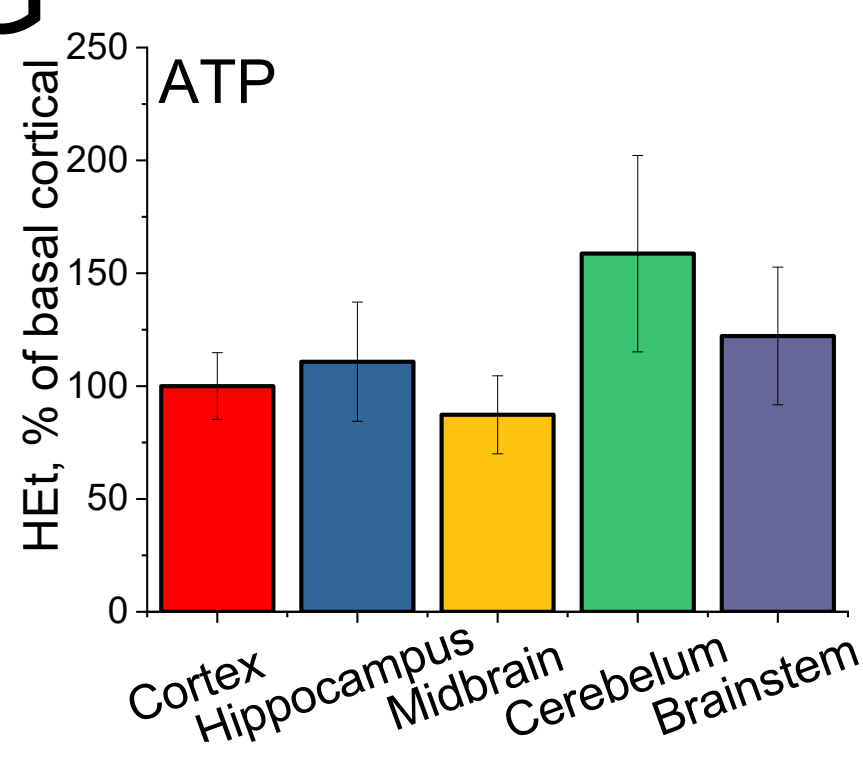
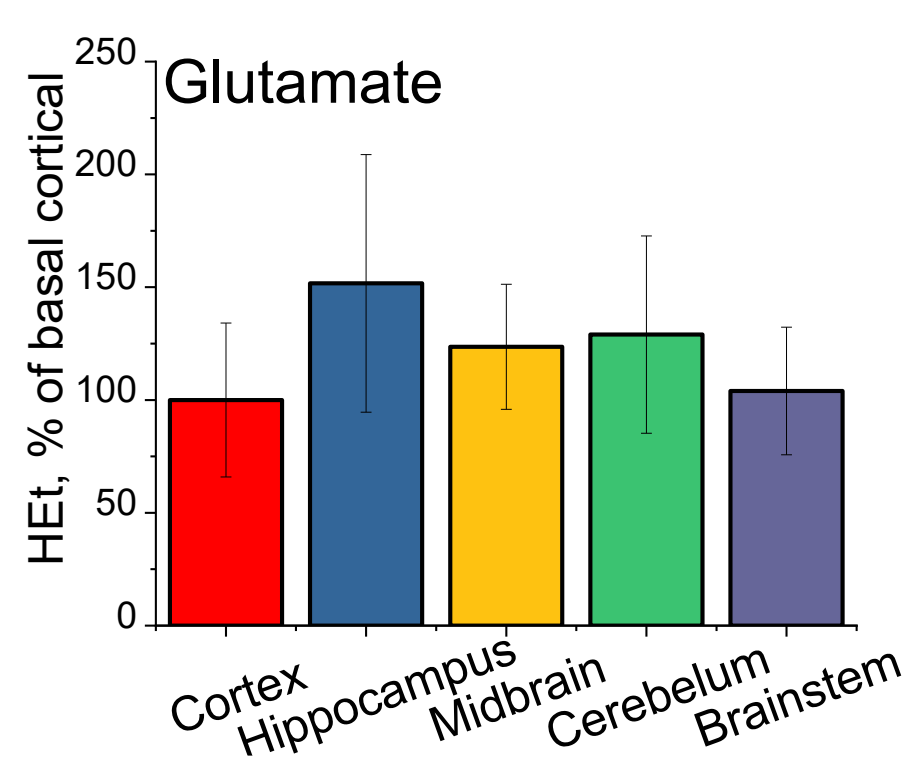
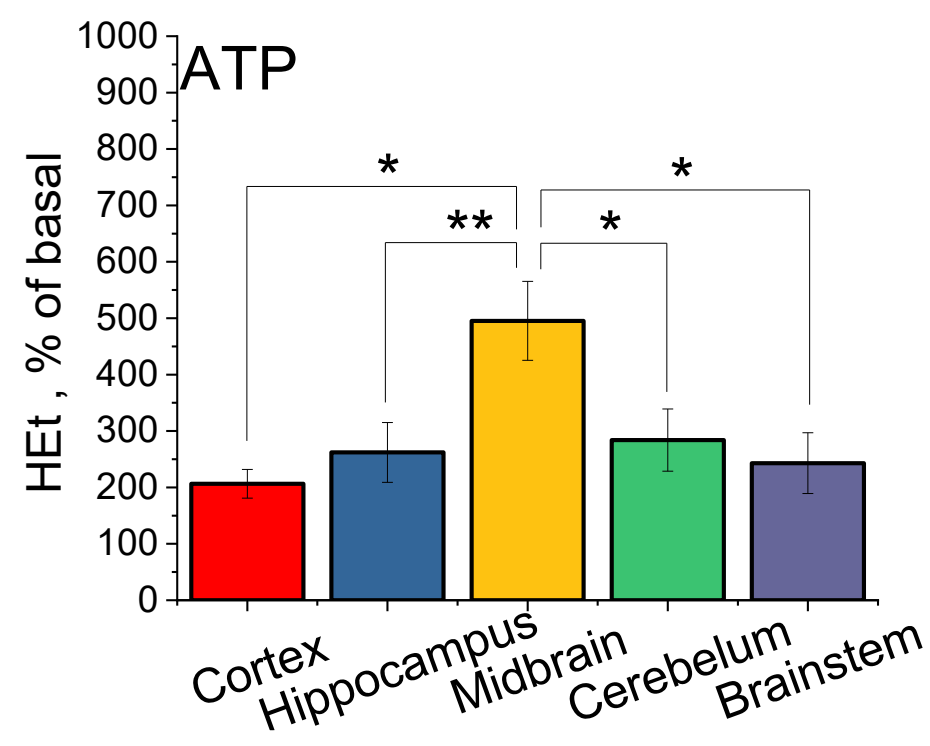
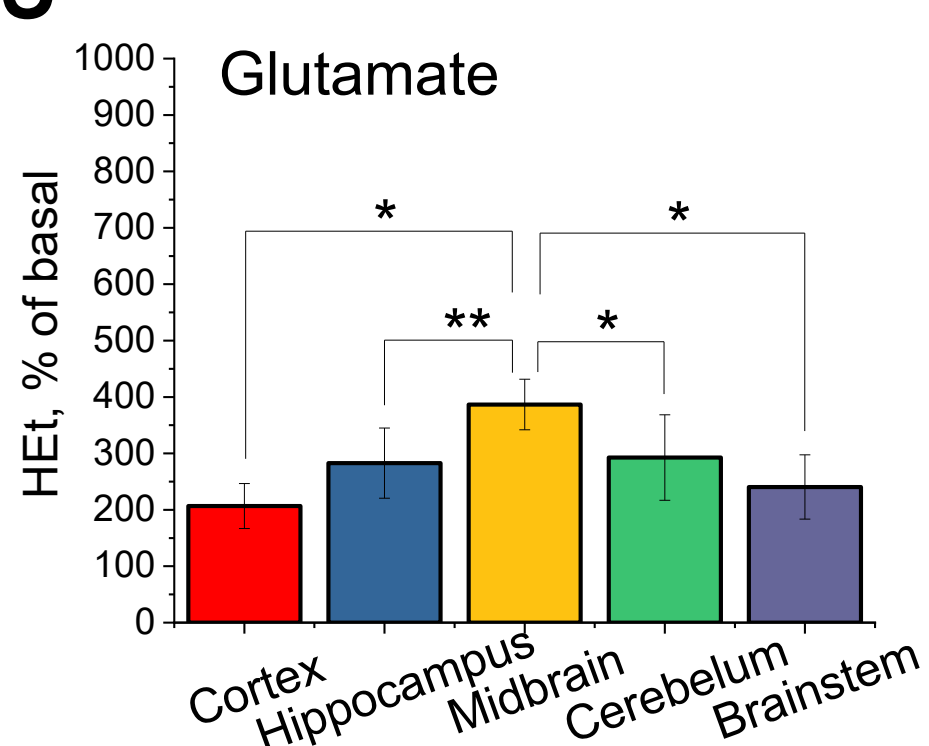
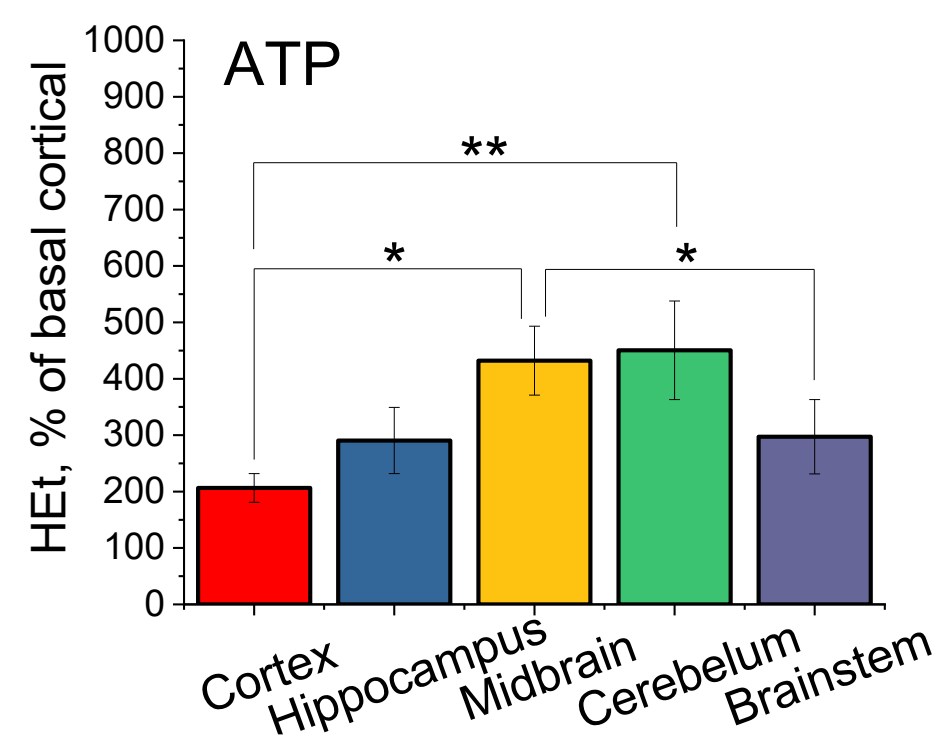
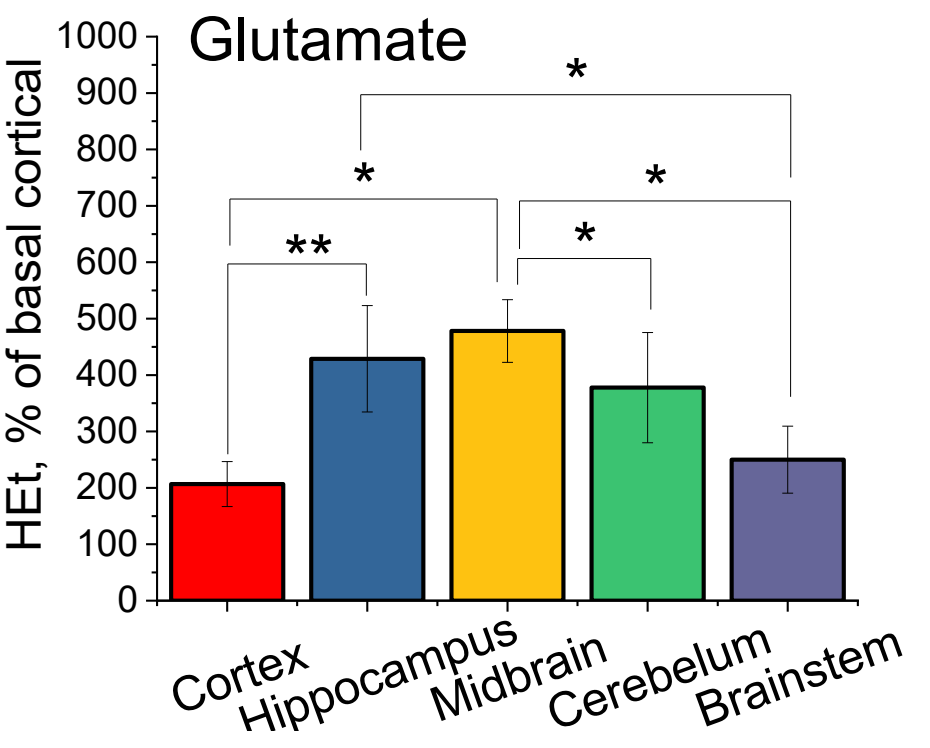
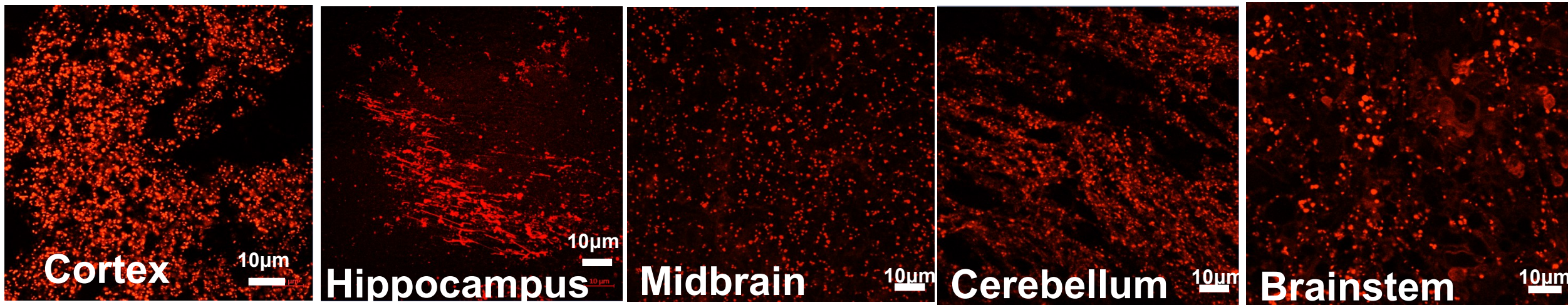
A**B****C****D****E****F****G**

Figure 1

A**B****C****D****E****F****G****H****I****J****K****L****Figure 2**

A



B

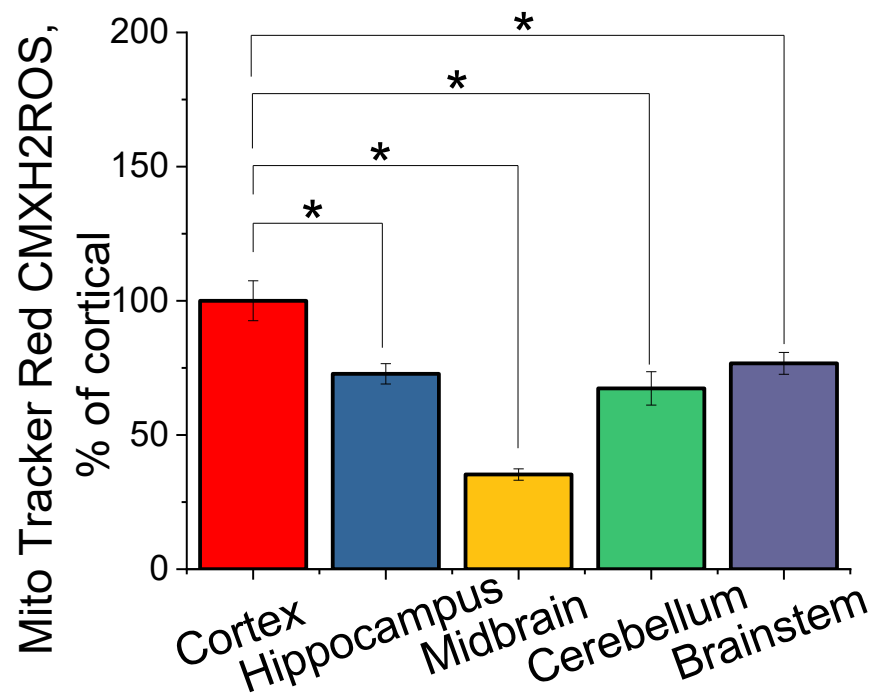


Figure 3

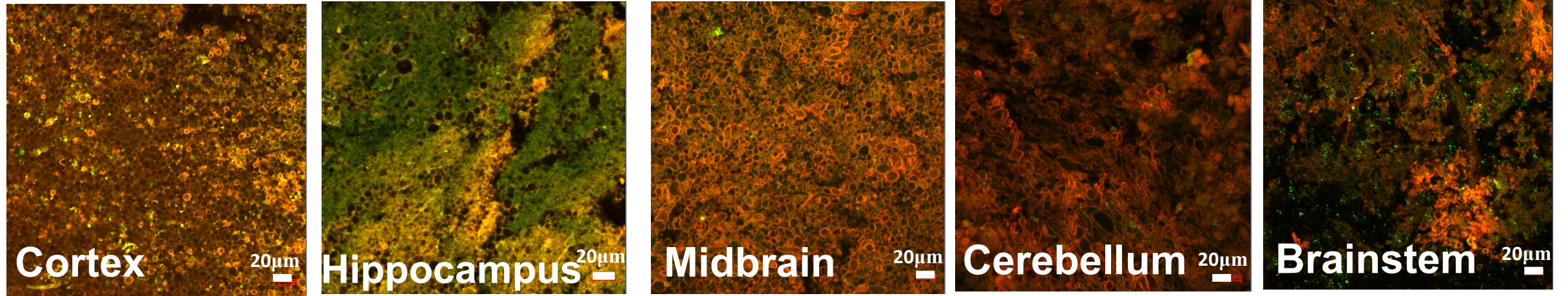
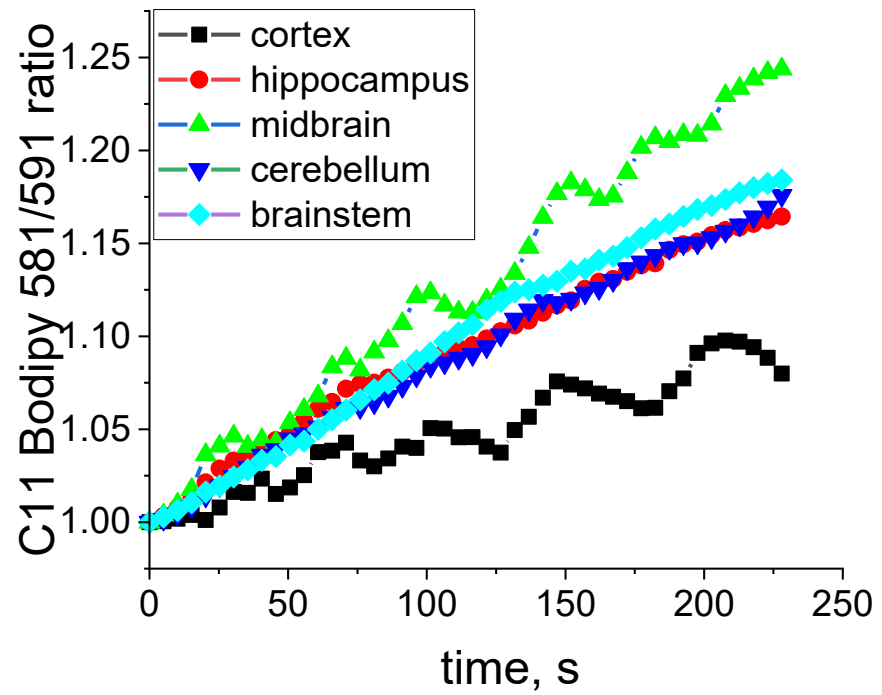
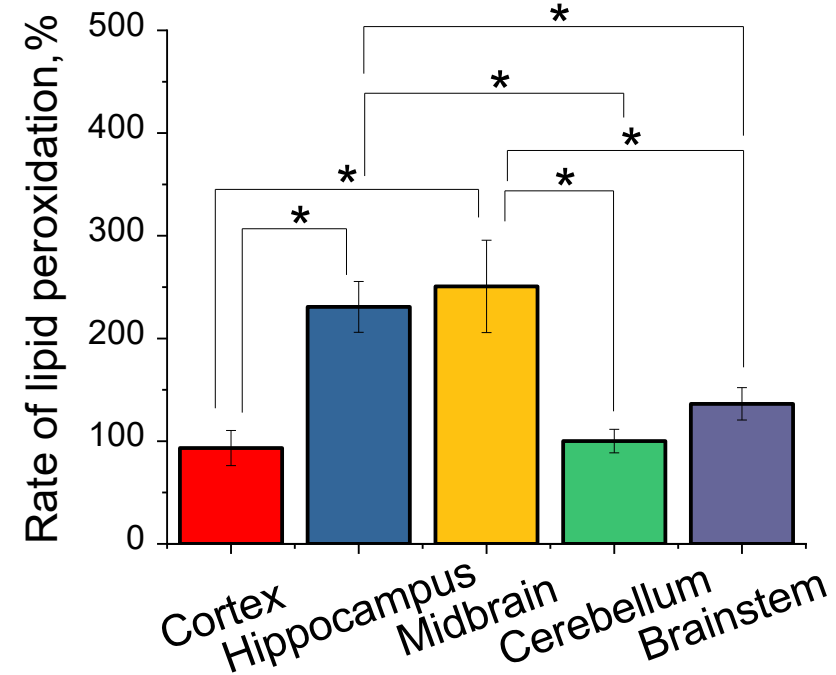
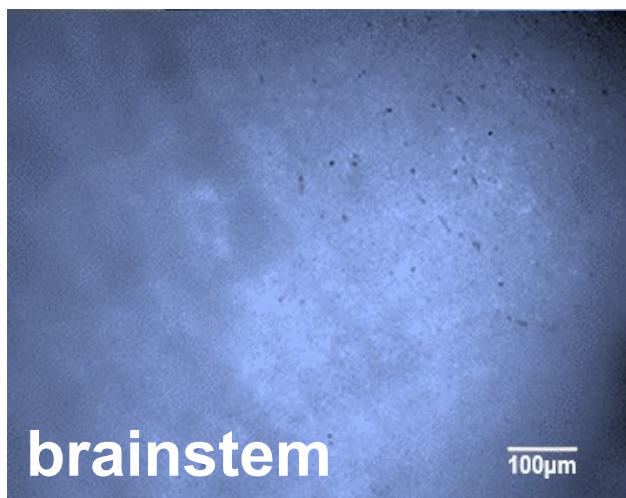
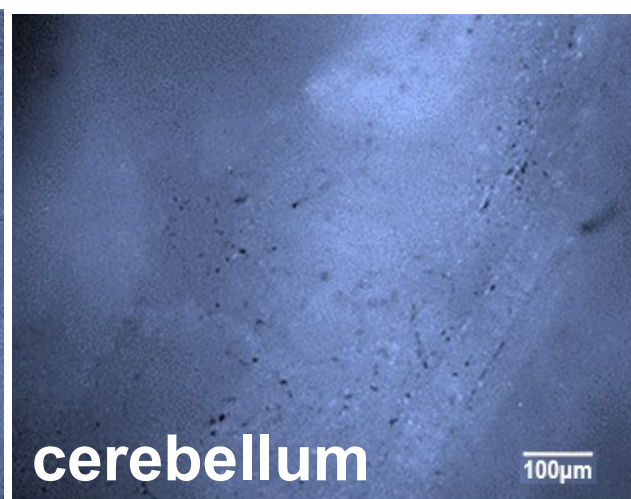
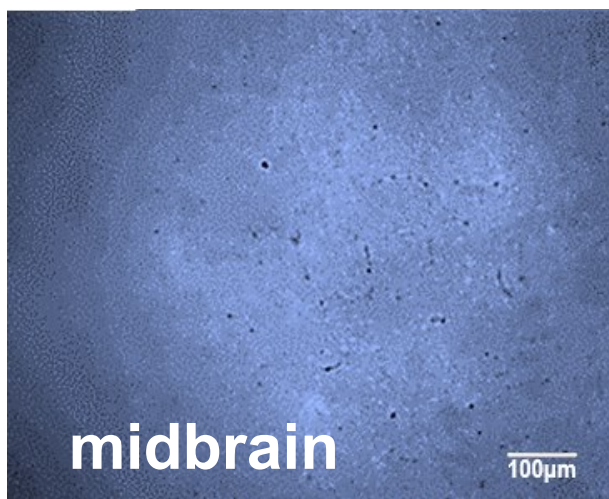
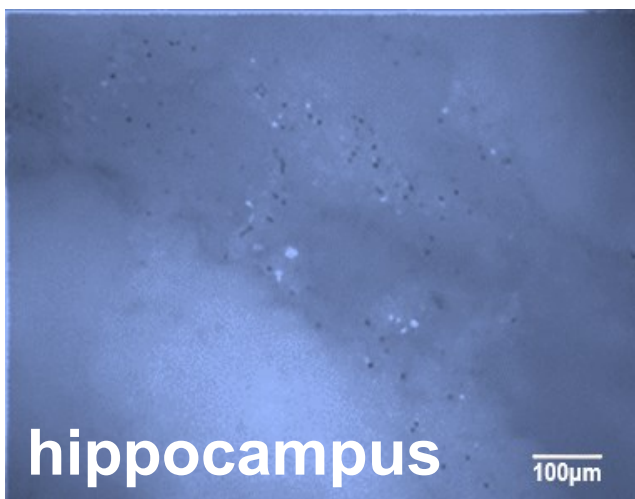
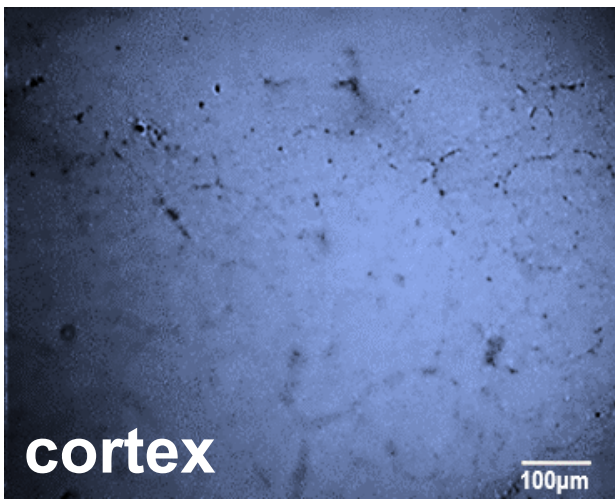
A**B****C**

Figure 4

A



B

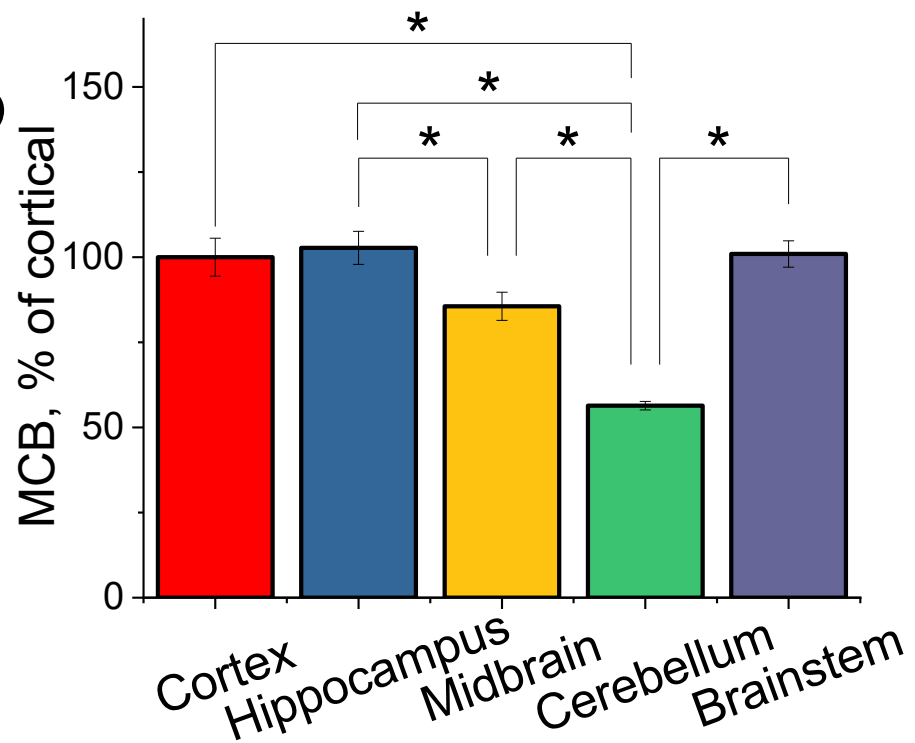


Figure 5